Lymph node fibroblastic reticular cells directly present peripheral tissue antigen under steady-state and inflammatory conditions

Anne L. Fletcher,[1] Veronika Lukacs-Kornek,[1] Erika D. Reynoso,[1,3] Sophie E. Pinner,[1] Angelique Bellemare-Pelletier,[1] Mark S. Curry,[2] Ai-Ris Collier,[1] Richard L. Boyd,[5] and Shannon J. Turley[1,4]

[1]Department of Cancer Immunology and AIDS and [2]Flow Cytometry Core Facility, Dana-Farber Cancer Institute, Boston, MA 02115
[3]Division of Medical Sciences and [4]Department of Pathology, Harvard Medical School, Boston, MA 02115
[5]Monash Immunology and Stem Cell Laboratories, Monash University, Clayton 3800, Australia

Lymph node stromal cells (LNSCs) can induce potent, antigen-specific T cell tolerance under steady-state conditions. Although expression of various peripheral tissue–restricted antigens (PTAs) and presentation to naive CD8$^+$ T cells has been demonstrated, the stromal subsets responsible have not been identified. We report that fibroblastic reticular cells (FRCs), which reside in the T cell zone of the LN, ectopically express and directly present a model PTA to naive T cells, inducing their proliferation. However, we found that no single LNSC subset was responsible for PTA expression; rather, each subset had its own characteristic antigen display. Studies to date have concentrated on PTA presentation under steady-state conditions; however, because LNs are frequently inflammatory sites, we assessed whether inflammation altered stromal cell–T cell interactions. Strikingly, FRCs showed reduced stimulation of T cells after Toll-like receptor 3 ligation. We also characterize an LNSC subset expressing the highest levels of autoimmune regulator, which responds potently to bystander inflammation by up-regulating PTA expression. Collectively, these data show that diverse stromal cell types have evolved to constitutively express PTAs, and that exposure to viral products alters the interaction between T cells and LNSCs.

CORRESPONDENCE
Shannon Turley:
Shannon_Turley@dfci.harvard.edu

Abbreviations used: AFP, α fetoprotein; Aire, autoimmune regulator; BEC, blood endothelial cell; DN, double negative; ECM, extracellular matrix; eTAC, extrathymic *Aire*-expressing cell; FRC, fibroblastic reticular cell; iFABP, intestinal fatty acid–binding protein; LEC, lymphatic endothelial cell; LNSC, LN stromal cell; mTEC, medullary thymic epithelial cell; PLP, proteolipid protein; PTA, peripheral tissue–restricted antigen; QPCR, quantitative PCR; TLR, Toll-like receptor; tOVA, truncated OVA; Tyr, tyrosinase.

Autoreactive T cells are ubiquitous to the normal lymphocyte repertoire, presumably to maximize potential immune responses to pathogens. In healthy individuals, peripheral tolerance mechanisms keep these cells in check to prevent autoimmunity.

The role of nonhematopoietic LN stromal cells (LNSCs) in peripheral tolerance is an emerging, quickly evolving field of study. Various groups have shown that LNSCs shape the T cell repertoire under noninflammatory conditions. In the steady state, they express a range of clinically relevant peripheral tissue–restricted antigens (PTAs; Lee et al., 2007; Nichols et al., 2007; Magnusson et al., 2008) and transcription factors (Gardner et al., 2008; Yip et al., 2009), and are highly effective at tolerizing autoreactive T cells (Lee et al., 2007; Nichols et al., 2007; Gardner et al., 2008; Magnusson et al., 2008). Reactive CD8$^+$ T cells are activated, induced to proliferate, and lost from the peripheral T cell pool (Lee et al., 2007; Nichols et al., 2007; Gardner et al., 2008; Magnusson et al., 2008).

Although bone marrow chimeras show that tolerance requires nonhematopoietic cells in these systems (Lee et al., 2007; Nichols et al., 2007; Gardner et al., 2008; Magnusson et al., 2008), the LN stromal niche is heterogeneous and poorly studied. As such, identification of the tolerizing cell type is difficult, requiring mice with a genetic trace for stromal lineages, or the ability to isolate these rare cells with high efficiency and purity.

The primary hypothesis regarding the identity of a tolerogenic LNSC suggests analogy to medullary thymic epithelial cells (mTECs), which express a wealth of PTAs (Derbinski et al., 2001;

The Rockefeller University Press $30.00
J. Exp. Med. Vol. 207 No. 4 689-697
www.jem.org/cgi/doi/10.1084/jem.20092642

The Journal of Experimental Medicine

Anderson et al., 2002) and tolerize the developing T cell repertoire. However, although Lee et al. (2007) reported expression of an intestinal PTA by a gp38$^+$ LNSC, Gardner et al. (2008) identified a tolerogenic gp38$^-$ stromal cell type. Each subset shared markers with mTECs.

In this report, we show that fibroblastic reticular cells (FRCs) endogenously express PTAs and directly stimulate naive antigen-specific CD8$^+$ T cells. We also report that lymphatic endothelial cells (LECs) are the only LNSC to express the melanocyte-associated enzyme tyrosinase (Tyr), suggesting an important contribution to peripheral tolerance, because LN expression of this PTA is crucial for deleting Tyr-specific T cells from the normal repertoire (Nichols et al., 2007). We further report that LNSC subsets respond to signaling through Toll-like receptor 3 (TLR3), with FRCs showing a reduced capacity to stimulate T cells. We also characterize a hitherto unstudied stromal subset, which showed unique up-regulation of PTAs and autoimmune regulator (Aire) in response to inflammation. These results carry novel implications for peripheral tolerance theory, showing that cells of highly diverse lineage, phenotype, and function can express PTAs and shape the T cell repertoire.

RESULTS AND DISCUSSION

The LN stromal compartment consists of discrete subsets

The LN stromal niche supports leukocyte entry, exit, migration, survival, and activation (Gretz et al., 1996; Katakai et al., 2004; Bajénoff et al., 2006; Link et al., 2007). Multiple opportunities therefore exist for tolerogenic interactions between T cells and stroma. With many studies emphasizing the biological, pathological, and therapeutic implications of a resident cell type that naturally deletes T cells in an antigen-specific manner (Lee et al., 2007; Nichols et al., 2007; Gardner et al., 2008; Magnusson et al., 2008; Reynoso et al., 2009; Yip et al., 2009), identification of the cells responsible is increasingly crucial. Limiting factors include the rarity of LNSCs, the collagen-rich structure of the LN, requiring enzymatic digestion, and sparse phenotypic and functional data.

By flow cytometry, nonhematopoietic LNSCs form four subsets based on expression of gp38 and CD31 (Fig. 1 A; Link et al., 2007). FRCs (gp38$^+$CD31$^-$) are the major stromal subset in skin-draining LNs, and provide survival factors and directional support for DCs and lymphocytes, which crawl along FRC meshwork to reach intra-LN niches (Katakai et al., 2004; Bajénoff et al., 2006; Link et al., 2007). T cell entry to and exit from LNs is regulated by blood endothelial cells (BECs; CD31$^+$gp38$^-$) and LECs (gp38$^+$CD31$^+$). FRCs, BECs, and LECs comprise 80–85% of nonhematopoietic LN cellular content. The double-negative (DN) population expresses neither gp38 nor CD31 (Fig. 1 A) and has not previously been characterized. In our hands, follicular DCs, which are confined to B cell zones, comprised <1% of CD45$^-$ stroma. Because of their rarity, these cells were not further characterized in this study.

In assessing the LNSC phenotype, we found that FRCs showed strong expression of VCAM-1 (a ligand for VLA-4 and α4β7 integrins expressed by lymphocytes), CD140a (common to mesenchymal fibroblasts), and CD44 (a matrix metalloproteinase dock, heparin sulfate proteoglycan, and hyaluronate receptor often expressed by fibroblastic cells; Fig. 1 B). LECs and BECs shared a similar phenotype, with

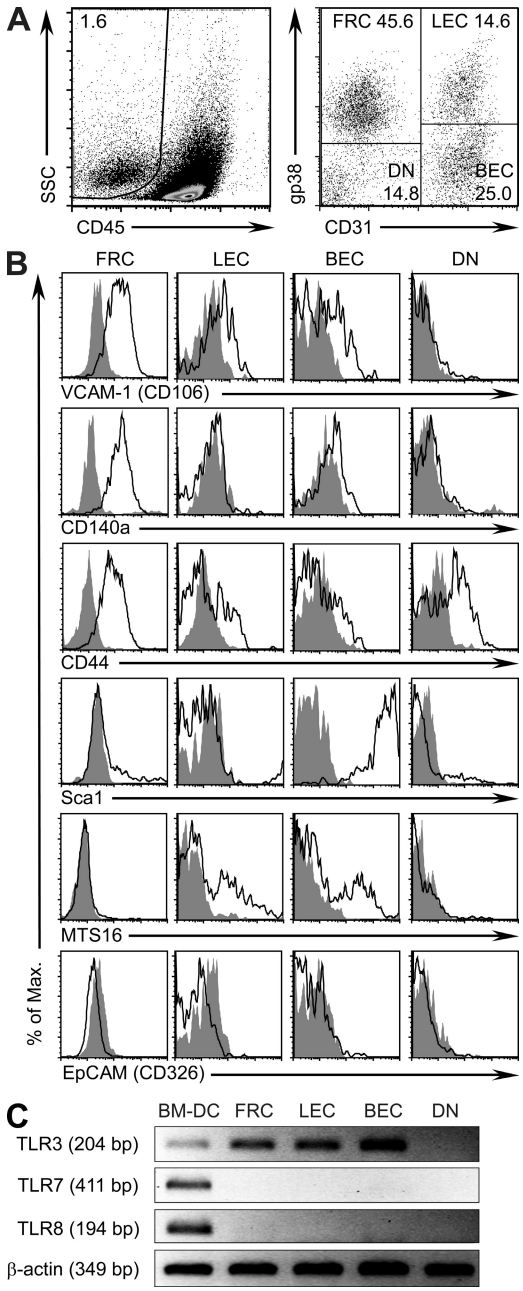

Figure 1. LNSC subsets are phenotypically distinct. (A) Flow cytometric strategy used to identify and sort CD45$^-$ LNSC subsets according to gp38 and CD31 expression. The percentage of CD45$^-$ stroma (left) and LNSC subsets (right) is shown. (B) LNSC subsets were analyzed using flow cytometry. Shading indicates isotype control. Data represent five to six mice from three experiments. (C) TLR expression in sorted LNSC subsets assessed by RT-PCR. Images represent three experiments. BM-DC, bone marrow–derived DC; SSC, side scatter.

low levels of VCAM-1 and a CD44-low subset. A distinct subset of LECs and BECs was stained by MTS16 (Fig. 1 B; Godfrey et al., 1990). In the thymus, MTS16 stains extracellular matrix (ECM) with similar reactivity to ER-TR7, an antibody that also stains FRCs; however, FRCs did not stain with MTS16, suggesting qualitative differences in ECM produced by thymus and LN fibroblastic cells. BECs uniquely expressed high levels of Sca-1 (Fig. 1 B), associated with self-renewal and ECM remodeling (Bonyadi et al., 2003; Kafadar et al., 2009). DN cells resembled FRCs in the level of CD44 and Sca-1 expression but lacked other fibroblastic markers such as CD140a (Fig. 1 B).

We did not detect epithelial cell adhesion molecule in LNSCs in C57BL/6 mice either by flow cytometry (Fig. 1 B) or quantitative PCR (QPCR; not depicted). Although Gardner et al. (2008) identified an epithelial cell adhesion molecule$^+$ Aire$^+$ cell type in LNs (termed extrathymic *Aire*-expressing cells [eTACs]), their low frequency compared with other stroma, high motility, and the fact that a genetic tracer is required to identify them makes them difficult to compare with classical nonmotile stroma. In addition, the *Adig* transgenic mice were bred on a nonobese diabetic mouse background, and these eTACs may differ in phenotype or frequency from those in other strains. In accordance with Hubert et al. (2008), we did not observe Aire protein expression (unpublished data). We were thus unable to identify eTACs in our preparations; these cells are likely too rare in nonautoimmune mice or express protein at levels too low to identify without a genetic reporter system.

Because virally infected FRCs have been linked to reduced CD8$^+$ T cell immunopathology (Mueller et al., 2007), we investigated expression of viral-associated TLRs in LNSC subsets. TLRs are critical components of the innate immune system that enable cells to detect highly conserved moieties associated with pathogen exposure. All classes of professional APCs express TLRs; however, in an unexplained paradox, there is precedence for TLR expression in stromal cell types associated with a microenvironment that is tolerogenic or poorly immunogenic. This includes intestinal epithelium, bone marrow–derived mesenchymal stromal cells, nonparenchymal liver cells, and ocular epithelial cells (Cario et al., 2000; Ueta et al., 2004; Wu et al., 2007; Liotta et al., 2008). Given substantial evidence that LNSCs are also primarily tolerogenic and may be immunosuppressive, even when virally infected (Mueller et al., 2007), we investigated TLR expression in LNSC subsets.

In the steady state, FRCs, LECs, and BECs expressed TLR3 (Fig. 1 C), which detects double-stranded RNA produced either as primary genetic material or as a replicative intermediate in most viral infections (Weber et al., 2006). DN cells uniquely lacked expression of all viral-associated TLRs. No stromal subsets expressed TLR7 or 8, which detect single-stranded RNA, using bone marrow–derived DCs as a positive control. Expression of TLR3 suggests that FRCs, LECs, and BECs are capable of directly responding to viral infection.

FRCs directly present a model peripheral tissue antigen to naive T cells

We have previously shown that an unknown component of nonhematopoietic stroma deletes autoreactive T cells in the intestinal fatty acid–binding protein (iFABP)–truncated OVA (tOVA) mouse model, where LNSCs express tOVA as a model PTA under the control of the tissue-specific promoter for iFABP (Lee et al., 2007). Robust proliferation of naive OT-I T cells is induced within 2 d after their transfer into iFABP-tOVA but not C57BL/6 hosts (Fig. 2 A), even when hematopoietic cells cannot present antigen (Lee et al., 2007). However, the nature of these initial experiments did not permit identification of the stromal subset responsible. By sorting FRC, LEC, BEC, and DN subsets to high purity and examining mRNA expression, we were able to identify FRCs as the stromal cell type predominantly responsible for tOVA expression in the iFABP-tOVA model (Fig. 2 B). Low transcript was evident in LEC, BEC, and DN subsets at high PCR cycle number (>45 cycles), which was not the result of contamination, because other FRC-restricted transcripts identified (see Fig. 3) could not be amplified from these subsets. Expression in FRCs was 40-fold higher than LECs, 73-fold higher than BECs, and 14-fold higher than DNs (unpublished data).

In vivo, naive OT-I T cells responding to tOVA presented by LNSCs in iFABP-tOVA mice strongly proliferate and are subsequently deleted, inducing tolerance (Lee et al., 2007). We conducted an in vitro stimulation assay and found that FRCs from iFABP-tOVA mice, but not C57BL/6 mice, induced division of OT-I T cells (Fig. 2 C). Up to 85% of the OT-I T cells up-regulated CD25, an early activation marker (Fig. 2 D). FRCs therefore present tOVA at levels high enough to functionally interact with T cells, inducing proliferation as seen before their deletion in vivo (Lee et al., 2007). This is the first demonstration that FRCs can act as APCs in LNs.

Interestingly, T cells stimulated by FRCs showed lower expression of CD25 compared with those stimulated by peptide-pulsed splenocytes (Fig. 2 C). A reduction in IL-2R may indicate a reduced capacity to respond to IL-2, reflecting the functional juxtaposition resulting from these interactions (activation versus eventual deletion). This, as well as any other difference in stimulated T cells, warrants further study.

Each LNSC subset has a unique PTA expression signature

A prominent hypothesis (Lee et al., 2007; Nichols et al., 2007; Gardner et al., 2008; Yip et al., 2009) suggests that a stromal subset analogous to thymic mTECs could bear the responsibility of PTA expression and tolerance induction in LNs. We assessed expression of representative PTAs in sorted LNSC subsets (Fig. 3). To our surprise, no single subset was responsible for PTA expression. Even antigens primarily expressed in melanocytes showed differential expression in LNSCs: although FRCs were the only cells expressing Mlana, only LECs expressed Tyr. Both proteins are current immunotherapy targets for melanoma (Trefzer et al., 2006). This finding had clinical relevance, because Tyr-reactive T cells escape

negative selection in the thymus; tolerance to this self-antigen relies on its expression by a nonhematopoietic cell in LNs (Nichols et al., 2007), and we identify that cell type as a LEC. It will be of the utmost clinical significance to determine whether PTA expression in LECs occurs by mechanisms specific to LN endothelium or is a property of lymphatic endothelium in general. Retinal S antigen was primarily expressed in BECs, although FRCs showed consistent, low transcript, while Rrad, a pancreas-associated PTA controlled by Aire in the spleen (Gardner et al., 2008), was expressed in all LNSC subsets. α Fetoprotein (AFP) and proteolipid protein (PLP), respectively associated with the liver and central nervous system, were similarly expressed in all LNSC subsets. Interestingly, QPCR showed that expression of Aire was predominant (~60-fold higher) in DNs (Fig. 3 B), with expression in FRCs, LECs, and BECs at the limits of detection. In two out of four sets of template, Aire was not detected in sorted BECs. Conversely, the Aire-like transcriptional modulator Deaf-1 was equally expressed in all skin-draining LNSCs (Fig. 3, A and B). Deaf-1 drives PTA expression in pancreatic LNs (Yip et al., 2009), and its reduction is associated with type I diabetes in humans and mice. Comparison of expression in primary tissue (Fig. 3 C) showed that FRCs expressed Mlana at levels equivalent to a melanocyte-enriched skin preparation, whereas PLP was 200-fold higher in the spinal cord compared with FRCs, and AFP, which is expressed by the liver at a low basal level after birth but increases after liver carcinoma or viral hepatitis, was expressed almost 100-fold lower in parenchyma-enriched adult mouse liver compared with FRCs.

Activation through TLR3 reduces FRC-mediated T cell stimulation

A prevailing view of tolerance states that DCs are primarily tolerogenic in the steady state but become profoundly

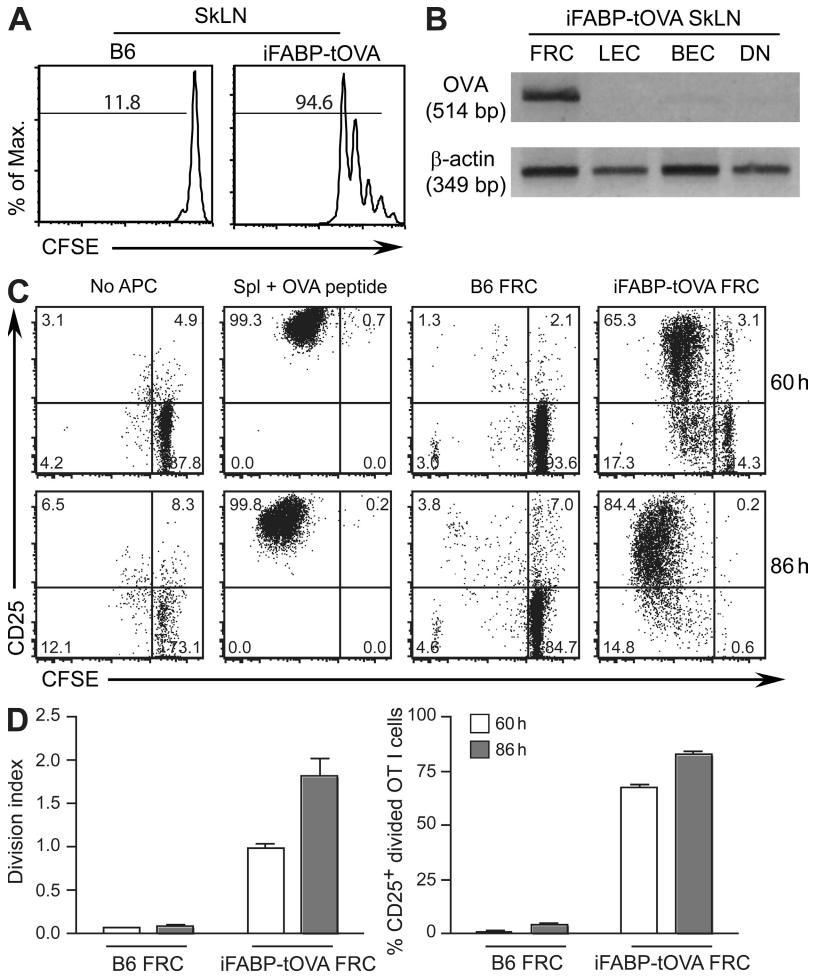

Figure 2. FRCs ectopically express and present OVA to OT-I T cells. (A) CFSE-labeled OT-I T cells were transferred into B6 or iFABP-tOVA hosts. T cell division, measured as the percentage of CFSE dilution, was assessed by flow cytometry. Graphs represent 12 mice from four experiments. (B) OVA transcription was assessed by RT-PCR. β-Actin was used to demonstrate cDNA integrity. Images are representative of three experiments. (C) Proliferation of CFSE-labeled OT-I T cells (shown as the percentage divided) was assessed after culture alone, with SIINFEKL-pulsed splenocytes, or with FRCs purified from C57BL/6 or iFABP-tOVA mice. Plots represent three experiments. (D) The cell division index (left) and proportion of divided cells (right) were calculated from three experiments. Graphs depict means + SD. SkLN, skin-draining LN.

immunostimulatory after exposure to "danger" signals such as tissue damage or microbial products. Although LNSC subsets similarly appear tolerogenic in the steady state, their function in an inflammatory milieu has not been formally tested. Expression of TLR3 in FRCs, LECs, and BECs suggests the capacity to respond directly to viral threat.

We injected mice with PolyI:C, which signals through TLR3. The reaction of LNSCs to viral infection is of particular interest, given that Mueller et al. (2007) showed that infection of FRCs correlated with viral persistence. It was unclear whether immunosuppression was intrinsic to FRCs under inflammatory conditions or whether the virus was subverting FRC function.

Because inflammation induces an escalatory effect within LNs, we tested stromal phenotype after PolyI:C injection at a relatively early time point (16 h) just sufficient for translation of co-stimulatory receptors, based on the response of $TLR3^+$ DCs. At this time point, DCs were in the process of up-regulating MHC class I, CD40, CD80, CD86, and PD-L1 (Fig. 4 A).

Control (PBS-injected) mice showed steady-state expression of CD40 and PD-L1 in all LNSC subsets, and CD80 was low in all subsets except LECs. CD86 was not expressed (Fig. 4 A). After PolyI:C injection, FRCs strongly up-regulated MHC class I and showed some increase in CD80 and CD86, whereas LECs up-regulated only CD80, and BECs showed no alteration of co-stimulatory receptors (Fig. 4 A). DN cells showed a modest increase in CD86 expression. However, the strongest response across all LNSC subsets occurred with PD-L1 (Fig. 4 A), the strongest prognostic indicator of deletion after interactions between T cells and LNSCs in experimental models of inflammation and autoimmunity (Mueller et al., 2007; Reynoso et al., 2009). Indeed, blocking PD-1 signal is sufficient to break the robust T cell tolerance normally induced after interaction between OT-I T cells and OVA-expressing LNSCs, causing autoimmunity (Reynoso et al., 2009).

Increased expression of CD86 and PD-L1 on DN cells showed that these phenotypic alterations could occur indirectly (because DN cells are $TLR3^-$), probably through inflammatory mediators from $TLR3^+$ cells. To test the net outcome of up-regulated MHC and co-stimulatory molecules balanced against a large increase in PD-L1, we tested the capacity of PolyI:C-treated iFABP-tOVA FRCs to stimulate OT-I T cells in vitro. Strikingly, FRCs were less capable of stimulating OT-I T cell division, whereas peptide-pulsed

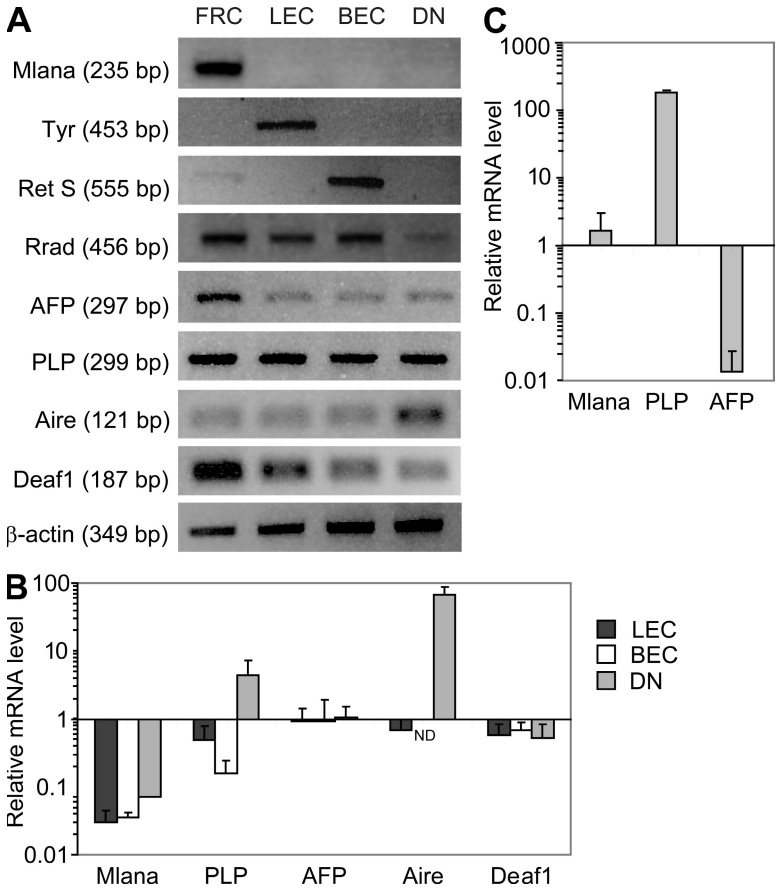

Figure 3. LNSC subsets show distinct PTA expression patterns. (A) RT-PCR was performed for a panel of PTAs. Images represent two to four experiments. (B) QPCR was performed for selected PTAs and transcriptional regulators. (C) QPCR was used to examine PTA expression in primary tissue compared with FRCs (normalized to 1, relative to GAPDH). All QPCR data show expression calculated relative to GAPDH and are depicted as fold change relative to FRCs, normalized to 1. All graphs depict means + SD from three to four experiments. ND, not detected; Ret S, retinal S antigen.

hematopoietic cells were not affected (Fig. 4, B and C). However, DCs and FRCs showed similar phenotypic changes in PD-L1, MHC class I, and co-stimulatory molecules after PolyI:C treatment (Fig. 4 A). These did not, therefore, account for the altered FRC–T cell interaction after PolyI:C exposure. Instead, we found that OVA expression was reduced sevenfold in FRCs sorted from PolyI:C-treated mice (Fig. 4 D), suggesting a possible mechanism for the reduced antigen-specific T cell stimulation observed. This was not the result of broadly reduced gene transcription, because FRCs did not down-regulate expression of all PTAs (Fig. 4 E). Although the outcome for a T cell recognizing a non–down-regulated PTA on a PolyI:C-treated FRC is unknown, at least one other study suggests that FRCs are tolerogenic after direct exposure to virus (Mueller et al. 2007).

The functional impact on T cells is the subject of further study, but it is apparent that the tolerogenic capacity of stroma is altered upon viral exposure. A mechanism similar to activation of tolerogenic DCs may occur, where administering TLR ligands alters the ability of DCs to stimulate T cells without compromising tolerance (Hamilton-Williams et al., 2005). OT-I T cells activated by TLR-stimulated DCs could not

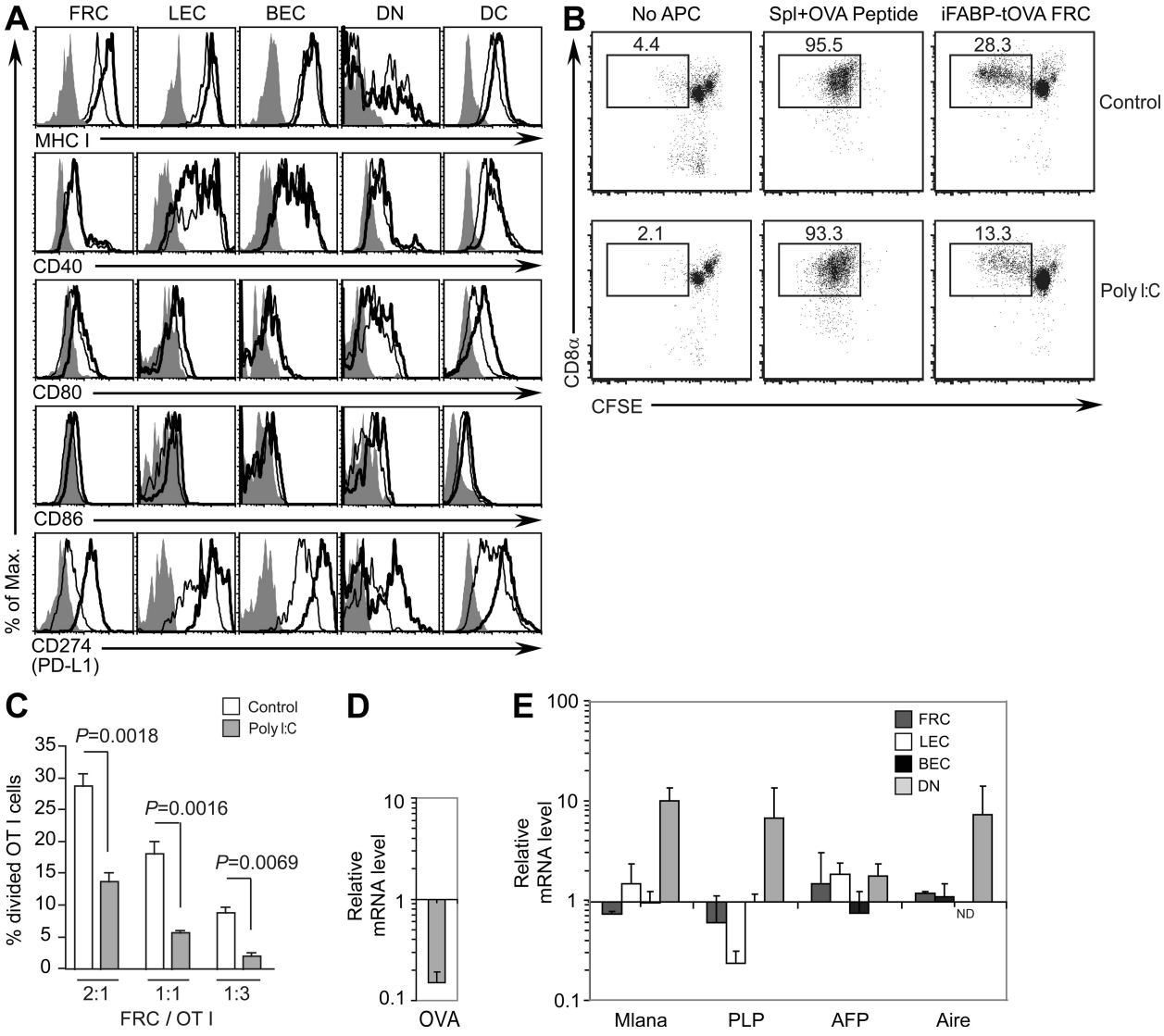

Figure 4. Activation through TLR3 alters LNSC phenotype and reduces FRC–mediated T cell stimulation. (A) LNSC expression of co-stimulatory and inhibitory receptors was assessed by flow cytometry. Plots represent six to seven mice from two to three experiments. Shading indicates isotype control; thin and thick lines depict data from PBS- or PolyI:C-treated mice, respectively. (B) Proliferation of CFSE-labeled OT-I T cells (shown as percentage divided) with and without PolyI:C. Cells were cultured without APCs, with SIINFEKL-pulsed splenocytes, or with FRCs purified from iFABP-tOVA mice. Plots represent three experiments. (C) OT I cell division was calculated across FRC/T cell dilutions. Graph depicts mean + SD from three experiments. (D) OVA expression levels in FRCs were assessed by QPCR after PolyI:C or PBS treatment of iFABP-tOVA mice. Graph depicts mean + SD from three experiments. (E) QPCR was performed for selected PTAs. Graph depicts mean + SD from two to three experiments. For all QPCR data, expression in PolyI:C-treated mice was calculated relative to GAPDH and depicted as fold change relative to expression in the appropriate subset from PBS-injected mice, normalized to 1. ND, not detected.

induce autoimmunity unless present at very high frequency and with $CD4^+$ T cell help (Hamilton-Williams et al., 2005).

Although tolerance in the iFABP-tOVA model is primarily deletional, residual OT-I T cells retain the ability to induce intestinal disease if cross-primed during an unrelated inflammatory process (Vezys et al., 2000; Vezys and Lefrançois, 2002). Up-regulation of PD-L1 may decrease the chance of this occurring. Cross-priming in this model has also been linked to CD40 activation, and it is striking that, of all the co-stimulatory molecules tested, LNSCs uniformly lack any change in CD40 expression in response to inflammation (Vezys and Lefrançois, 2002).

Collectively, these data paint a far more intricate picture of LNSC-mediated tolerance than previously appreciated. We show that LN FRCs express PTAs and can act as effective APCs for naive $CD8^+$ T cells, and that FRCs possess reduced capacity to stimulate T cells after TLR3 ligation. FRCs, LECs, and BECs all express virus-responsive TLR3, and LECs are the only LNSC subset to express Tyr, an antigen for which LNSC-based tolerance is crucial (Nichols et al., 2007). Tolerance to other PTAs, particularly retinal S antigen, which is strongly expressed by BECs, is yet to be demonstrated, but our results indicate that multiple stromal cell types are likely to contribute to peripheral tolerance.

The function, location, and lineage of the DN subset is unknown, but the evidence suggests that these cells are important components of the stromal niche, expressing the highest levels of Aire but lacking TLR3 expressed by DCs and other LNSC subsets, and showing a strong, unique response to inflammation by up-regulating PTA expression (Fig. 4 E). These cells will form the subject of further study.

It is striking that LNSCs should show reduced ability to stimulate T cells after contact with microbial products that signal a potential threat. There are two plausible reasons for this. The first is to prevent low-affinity autoreactive T cells from acquiring effector function during an immune response. The second is more crucial: to preserve LN structure and function during an immune response by preventing activation of $CD8^+$ T cells specific to viral antigens presented by stromal cells. Indeed, Mueller et al. (2007) reported that a lymphocytic choriomeningitis virus strain directly infecting FRCs was associated with reduced T cell–mediated damage to the structure of the LN. Clearly the tolerogenic capacity of these cells is not limited to endogenous PTAs. This makes them an attractive target for autoimmune and transplantation tolerance therapy. Finally, the expression of PTAs across stromal subsets of diverse primary function and lineage suggests that tolerance induction is not a specialist function in LNs, supporting and extending a recent parallel hypothesis that PTA expression may be a general function of all epithelium (Dooley et al., 2009). In this report, we show that in LNs, PTA expression is a responsibility shared between all parenchymal cell types.

MATERIALS AND METHODS

Mice. Male C57BL/6 mice aged 4–6 wk were obtained from the Jackson Laboratory; iFABP-tOVA mice were bred in house from the 232-4 transgenic mouse line generated by L. Lefrançois (University of Connecticut, Farmington, CT; Vezys et al., 2000). C57BL/6 OT-I TCR transgenic $Rag^{-/-}$ mice were obtained from Taconic. All mice were specific pathogen free and cared for in accordance with institutional and National Institutes of Health guidelines. Experimental procedures were conducted with the approval of the Research Animal Care subcommittee at the Dana-Farber Cancer Institute.

Stromal cell isolation and staining for flow cytometry. Skin-draining LNs (inguinal, axillary, and brachial) for each mouse were digested separately using 1 ml of enzyme mix containing 0.2 mg/ml Collagenase P (Roche), 0.1 mg/ml DNase I (Invitrogen), and 0.8 mg/ml Dispase (Roche) at 37°C for 15 min. Tissues were agitated, media were collected, and the digestion mix was replaced. This proceeded for 50–60 min, when LNs were completely digested. As previously described (Fletcher et al., 2009), 5×10^6 cells were stained, acquired on a FACSCalibur or FACSAria (BD), and analyzed using FlowJo software (Tree Star, Inc.).

Stromal cell enrichment and sorting. LNs from 6–10 mice per group were pooled for digestion, as detailed in the previous section, using 5 ml of enzyme mix. Cells were counted and filtered as described, and enriched for $CD45^-$ stroma as previously described (Fletcher et al., 2009). Stained cells were sorted using a FACSAria fitted with a 100-µm tip at a pressure of 20 psi. The purity of sorted stromal populations routinely exceeded 96%. Tail skin was digested for 90 min using enzyme mix, with fractions collected at 15-min intervals. Highly pigmented fractions enriched in melanocytes were retained for QPCR analysis. Spinal cord was digested to a single-cell suspension within 15 min; liver was digested and enriched for $CD45^-$ stroma similarly to LNs.

Treatment with PolyI:C. Mice were injected i.v. with either 100 µg PolyI:C (GE Healthcare) in PBS or PBS alone, and sacrificed for analysis after 16–18 h.

Analysis of T cell proliferation. For in vivo analysis, 4×10^6 CFSE-labeled OT-I T cells were transferred i.v. into C57BL/6 or iFABP-tOVA mice, and skin-draining LNs were analyzed 42 h later. For in vitro analysis, skin-draining LNs were enzymatically digested. $CD45^+$ and $CD31^+$ cells were depleted to high purity using MACS separation (Miltenyi Biotec). Remaining FRCs were cultured with CFSE-labeled OT-I T cells in culture media (αMEM; 10% FCS, 10 U/ml IL-2, 1% penicillin/streptomycin) with 2.5 µg/ml PolyI:C where indicated in the figures. As a positive control, splenocytes were incubated with 1 mg/ml SIINFEKL (AnaSpec). OT-I T cells were identified by TCR clonotype, and proliferation was measured using CFSE dilution. The division index was calculated as the mean number of divisions among cells that had divided at least once.

PCR. Preparation of sorted cells and cDNA synthesis were performed as previously described (Fletcher et al., 2009). The concentration of cDNA was adjusted to 250 nM for all subsets. Cycling conditions for PTA analysis were 95°C for 10 min, followed by 40 cycles of 95°C for 30 s, 54.5°C for 45 s, and 72°C for 45 s. For TLR analysis, PCR conditions were 94°C for 5 min, followed by 40 cycles of 94°C for 60 s, 55°C for 60 s, and 72°C for 1 min. QPCR was performed with 200 nM of validated primers in 25-µl reactions using the Platinum SYBR Green One-Step qPCR kit (Invitrogen) and the following program: 50°C for 2 min, 95°C for 10 min, and 40 cycles of amplification at 95°C for 15 s and 60°C for 60 s. Relative levels of target mRNA were compared with GAPDH using the $2^{-\Delta\Delta Ct}$ method, where the control cell type or treatment group was normalized to 1. Primers were obtained from Integrated DNA Technologies. Sequences were as follows: TLR3, (For) 5′-TTGTCTTCTGCACGAACCTG-3′ and (Rev) 5′-CGCAACGCAAGGATTTTATT-3′; TLR7, (For) 5′-TTCCGATACGATGAATATGCACG-3′ and (Rev) 5′-TGAGTTTGTCCAGAAGCCGTAAT-3′; TLR8, (For) 5′-GGCACAACTCCCTTGTGATT-3′ and (Rev) 5′-CATTTGGGTGCTGTTGTTTG-3′; B-actin, (For) 5′-TGGAATCCTGTGGCATCCATGAAAC-3′

and (Rev) 5′-TAAAACGCAGCTCAGTAACAGTCCG-3′; OVA, (For) 5′-CACAAGCAATGCCTTTCAGA-3′ and (Rev) 5′-GAATGGATGGTCAGCCCTAA-3′ or (For) 5′-GCAAACCTGTGCAGATGATG-3′ and (Rev) 5′-CACCAACATGCTCATTGTCC-3′; Mlana, (For) 5′-CTGCTGAAGAGGCCGCAGGG-3′ and (Rev) 5′-GGAGCGTTGGGAACCACGGG-3′; Tyr, (For) 5′-ATTGATTTTGCCCATGAAGC-3′ and (Rev) 5′-GGCAAATCCTTCCAGTGTGT-3′; retinal S antigen, (For) 5′-TGACTACCTACCCTGTTCAG-3′ and (Rev) 5′-TTCACTGGATGTGAGCTCTC-3′; Rrad, (For) 5′-GGGAACAGGATGGGGGCTGC-3′ and (Rev) 5′-TGGCGCGGAAGGCCATCTTG-3′; AFP, (For) 5′-GCTGTGGTGAGGGAATGGCCG-3′ and (Rev) 5′-CCGCCAGCTGCTCCTCTGTC-3′; PLP, (For) 5′-CAGGGGGCCAGAAGGGGAGG-3′ and (Rev) 5′-GCAGCACCCACAAACGCAGC-3′; Aire, (For) 5′-AGGCTCCCACCTGAAGACTAA-3′ and (Rev) 5′-CACGGTCACAGCTCTCTGG-3′; Deaf-1, (For) 5′-ACTCTGAGTGGCCCTGTCAG-3′ and (Rev) 5′-TGTCAAAGGTCAGTGCTCC-3′; and GAPDH, (For) 5′-AACTTTGGCATTGTGGAAGG-3′ and (Rev) 5′-ACACATTGGGGGTAGGAACA-3′.

Antibodies. Primary antibodies were as follows: CD45 (clone 30-F11), CD106 (clone 429), Sca-1 (clone D7), and PD-L1 (clone MIH5; BD); anti-CD31 (clone MEC13.3), MHC class I (clone 28-8-6), CD40 (clone HM40.3), CD80 (clone I6-10A1), CD44 (clone IM7), and CD8α (clone 53-6.7; BioLegend); and anti-CD140a (APA5) and CD25 (clone PC61.5; eBioscience). Anti-CD86 (clone RMMP-2) and Vα2 TCR (clone B20.1) were purchased from Invitrogen, and anti-CD326 (clone G8.8) was purchased from Santa Cruz Biotechnology, Inc. Clone MTS16 was created and grown in house. Anti-gp38 was purified in house from clone 8.1.1 obtained from the Developmental Studies Hybridoma Bank.

Statistical analysis. Statistical analysis was performed using Prism 4 for Macintosh (GraphPad Software, Inc.). Data were compared using an unpaired two-tailed *t* test with 95% confidence intervals.

This work was supported by National Institutes of Health grants R01 DK074500 and P01 AI045757 (to S.J. Turley), and a National Health Medical Research Council Postdoctoral Biomedical Training Fellowship (to A.L. Fletcher).

The authors have no conflicting financial interests.

Submitted: 10 December 2009
Accepted: 23 February 2010

REFERENCES

Anderson, M.S., E.S. Venanzi, L. Klein, Z. Chen, S.P. Berzins, S.J. Turley, H. von Boehmer, R. Bronson, A. Dierich, C. Benoist, and D. Mathis. 2002. Projection of an immunological self shadow within the thymus by the aire protein. *Science*. 298:1395–1401. doi:10.1126/science.1075958

Bajénoff, M., J.G. Egen, L.Y. Koo, J.P. Laugier, F. Brau, N. Glaichenhaus, and R.N. Germain. 2006. Stromal cell networks regulate lymphocyte entry, migration, and territoriality in lymph nodes. *Immunity*. 25:989–1001. doi:10.1016/j.immuni.2006.10.011

Bonyadi, M., S.D. Waldman, D. Liu, J.E. Aubin, M.D. Grynpas, and W.L. Stanford. 2003. Mesenchymal progenitor self-renewal deficiency leads to age-dependent osteoporosis in Sca-1/Ly-6A null mice. *Proc. Natl. Acad. Sci. USA*. 100:5840–5845. doi:10.1073/pnas.1036475100

Cario, E., I.M. Rosenberg, S.L. Brandwein, P.L. Beck, H.C. Reinecker, and D.K. Podolsky. 2000. Lipopolysaccharide activates distinct signaling pathways in intestinal epithelial cell lines expressing Toll-like receptors. *J. Immunol.* 164:966–972.

Derbinski, J., A. Schulte, B. Kyewski, and L. Klein. 2001. Promiscuous gene expression in medullary thymic epithelial cells mirrors the peripheral self. *Nat. Immunol.* 2:1032–1039. doi:10.1038/ni723

Dooley, J., M. Erickson, and A.G. Farr. 2009. Lessons from thymic epithelial heterogeneity: FoxN1 and tissue-restricted gene expression by extrathymic, endodermally derived epithelium. *J. Immunol.* 183:5042–5049. doi:10.4049/jimmunol.0901371

Fletcher, A.L., T.E. Lowen, S. Sakkal, J.J. Reiseger, M.V. Hammett, N. Seach, H.S. Scott, R.L. Boyd, and A.P. Chidgey. 2009. Ablation and regeneration of tolerance-inducing medullary thymic epithelial cells after cyclosporine, cyclophosphamide, and dexamethasone treatment. *J. Immunol.* 183:823–831. doi:10.4049/jimmunol.0900225

Gardner, J.M., J.J. Devoss, R.S. Friedman, D.J. Wong, Y.X. Tan, X. Zhou, K.P. Johannes, M.A. Su, H.Y. Chang, M.F. Krummel, and M.S. Anderson. 2008. Deletional tolerance mediated by extrathymic Aire-expressing cells. *Science*. 321:843–847. doi:10.1126/science.1159407

Godfrey, D.I., D.J. Izon, C.L. Tucek, T.J. Wilson, and R.L. Boyd. 1990. The phenotypic heterogeneity of mouse thymic stromal cells. *Immunology*. 70:66–74.

Gretz, J.E., E.P. Kaldjian, A.O. Anderson, and S. Shaw. 1996. Sophisticated strategies for information encounter in the lymph node: the reticular network as a conduit of soluble information and a highway for cell traffic. *J. Immunol.* 157:495–499.

Hamilton-Williams, E.E., A. Lang, D. Benke, G.M. Davey, K.H. Wiesmüller, and C. Kurts. 2005. Cutting edge: TLR ligands are not sufficient to break cross-tolerance to self-antigens. *J. Immunol.* 174:1159–1163.

Hubert, F.-X., S.A. Kinkel, K.E. Webster, P. Cannon, P.E. Crewther, A.I. Proeitto, L. Wu, W.R. Heath, and H.S. Scott. 2008. A specific anti-Aire antibody reveals aire expression is restricted to medullary thymic epithelial cells and not expressed in periphery. *J. Immunol.* 180:3824–3832.

Kafadar, K.A., L. Yi, Y. Ahmad, L. So, F. Rossi, and G.K. Pavlath. 2009. Sca-1 expression is required for efficient remodeling of the extracellular matrix during skeletal muscle regeneration. *Dev. Biol.* 326:47–59. doi:10.1016/j.ydbio.2008.10.036

Katakai, T., T. Hara, M. Sugai, H. Gonda, and A. Shimizu. 2004. Lymph node fibroblastic reticular cells construct the stromal reticulum via contact with lymphocytes. *J. Exp. Med.* 200:783–795. doi:10.1084/jem.20040254

Lee, J.W., M. Epardaud, J. Sun, J.E. Becker, A.C. Cheng, A.R. Yonekura, J.K. Heath, and S.J. Turley. 2007. Peripheral antigen display by lymph node stroma promotes T cell tolerance to intestinal self. *Nat. Immunol.* 8:181–190. doi:10.1038/ni1427

Link, A., T.K. Vogt, S. Favre, M.R. Britschgi, H. Acha-Orbea, B. Hinz, J.G. Cyster, and S.A. Luther. 2007. Fibroblastic reticular cells in lymph nodes regulate the homeostasis of naive T cells. *Nat. Immunol.* 8:1255–1265. doi:10.1038/ni1513

Liotta, F., R. Angeli, L. Cosmi, L. Filì, C. Manuelli, F. Frosali, B. Mazzinghi, L. Maggi, A. Pasini, V. Lisi, et al. 2008. Toll-like receptors 3 and 4 are expressed by human bone marrow-derived mesenchymal stem cells and can inhibit their T-cell modulatory activity by impairing Notch signaling. *Stem Cells*. 26:279–289. doi:10.1634/stemcells.2007-0454

Magnusson, F.C., R.S. Liblau, H. von Boehmer, M.J. Pittet, J.W. Lee, S.J. Turley, and K. Khazaie. 2008. Direct presentation of antigen by lymph node stromal cells protects against CD8 T-cell-mediated intestinal autoimmunity. *Gastroenterology*. 134:1028–1037. doi:10.1053/j.gastro.2008.01.070

Mueller, S.N., M. Matloubian, D.M. Clemens, A.H. Sharpe, G.J. Freeman, S. Gangappa, C.P. Larsen, and R. Ahmed. 2007. Viral targeting of fibroblastic reticular cells contributes to immunosuppression and persistence during chronic infection. *Proc. Natl. Acad. Sci. USA*. 104:15430–15435. doi:10.1073/pnas.0702579104

Nichols, L.A., Y. Chen, T.A. Colella, C.L. Bennett, B.E. Clausen, and V.H. Engelhard. 2007. Deletional self-tolerance to a melanocyte/melanoma antigen derived from tyrosinase is mediated by a radio-resistant cell in peripheral and mesenteric lymph nodes. *J. Immunol.* 179:993–1003.

Reynoso, E.D., K.G. Elpek, L. Francisco, R. Bronson, A. Bellemare-Pelletier, A.H. Sharpe, G.J. Freeman, and S.J. Turley. 2009. Intestinal tolerance is converted to autoimmune enteritis upon PD-1 ligand blockade. *J. Immunol.* 182:2102–2112. doi:10.4049/jimmunol.0802769

Trefzer, U., M. Hofmann, S. Reinke, Y.J. Guo, H. Audring, G. Spagnoli, and W. Sterry. 2006. Concordant loss of melanoma differentiation antigens in synchronous and asynchronous melanoma metastases: implications for immunotherapy. *Melanoma Res.* 16:137–145. doi:10.1097/01.cmr.0000200489.55099.20

Ueta, M., T. Nochi, M.H. Jang, E.J. Park, O. Igarashi, A. Hino, S. Kawasaki, T. Shikina, T. Hiroi, S. Kinoshita, and H. Kiyono. 2004. Intracellularly expressed TLR2s and TLR4s contribution to an immunosilent environment at the ocular mucosal epithelium. *J. Immunol.* 173:3337–3347.

Vezys, V., and L. Lefrançois. 2002. Cutting edge: inflammatory signals drive organ-specific autoimmunity to normally cross-tolerizing endogenous antigen. *J. Immunol.* 169:6677–6680.

Vezys, V., S. Olson, and L. Lefrançois. 2000. Expression of intestine-specific antigen reveals novel pathways of CD8 T cell tolerance induction. *Immunity.* 12:505–514. doi:10.1016/S1074-7613(00)80202-2

Weber, F., V. Wagner, S.B. Rasmussen, R. Hartmann, and S.R. Paludan. 2006. Double-stranded RNA is produced by positive-strand RNA viruses and DNA viruses but not in detectable amounts by negative-strand RNA viruses. *J. Virol.* 80:5059–5064. doi:10.1128/JVI.80.10.5059-5064.2006

Wu, J., M. Lu, Z. Meng, M. Trippler, R. Broering, A. Szczeponek, F. Krux, U. Dittmer, M. Roggendorf, G. Gerken, and J.F. Schlaak. 2007. Toll-like receptor-mediated control of HBV replication by nonparenchymal liver cells in mice. *Hepatology.* 46:1769–1778. doi:10.1002/hep.21897

Yip, L., L. Su, D. Sheng, P. Chang, M. Atkinson, M. Czesak, P.R. Albert, A.R. Collier, S.J. Turley, C.G. Fathman, and R.J. Creusot. 2009. Deaf1 isoforms control the expression of genes encoding peripheral tissue antigens in the pancreatic lymph nodes during type 1 diabetes. *Nat. Immunol.* 10:1026–1033. doi:10.1038/ni.1773